

# Any immersion remote refocus (AIRR) microscopy

This project is maintained by amsikking in the York lab, and was funded by Calico Life Sciences LLC

## Appendix

---

Note that this is a limited PDF or print version; animated and interactive figures are disabled. For the full version of this article, please visit one of the following links:

[https://amsikking.github.io/any\\_immersion\\_remote\\_refocus\\_microscopy](https://amsikking.github.io/any_immersion_remote_refocus_microscopy)

---

## Any immersion remote refocus (AIRR) microscopy

---

[Back to the main text](#)

### Theory

---

Here we present the equations used in the results section to evaluate the widefield and remote refocus microscope design options.

#### **Numerical aperture and resolution**

The numerical aperture (NA) is defined as:

$$NA = n_i \sin \theta_i \tag{a1}$$

where  $n_i$  is the refractive index of the immersion medium and  $\theta_i$  is the collection half-angle of the objective. In the case of a planar refractive index boundary like a coverslip the NA is conserved via Snell's law:

$$n_s \sin \theta_s = n_i \sin \theta_i \tag{a2}$$

where  $n_s$  is the refractive index of the sample and  $\theta_s$  is the collection half-angle in sample space. According to the Rayleigh criteria the smallest resolvable feature size  $r_{min}$  is then:

$$r_{min} = 0.61 \frac{\lambda}{NA} \quad (a3)$$

where  $\lambda$  is the wavelength of the collected light [Pawley 2006].

### Focal length, field of view and pixels

The objective lens focal length  $f$  is found with:

$$f = \frac{f_{TL}}{M} \quad (a4)$$

where  $f_{TL}$  is the tube lens focal length (200mm for Nikon) and  $M$  is the magnification of the objective. The sample space field of view (FOV) is then assumed to be:

$$FOV = \frac{FN}{M} \quad (a5)$$

where FN is the field number according to the manufacturer (20mm assumed for Nikon). When choosing an objective it can be useful to estimate the number of Nyquist pixels  $N_{px}$  the lens can deliver across the FOV for specifying a camera using:

$$N_{px} = 2 \frac{FOV}{r_{min}} \quad (a6)$$

Note: this can also serve as a measure of the *quality* of the objective, where more pixels usually indicates a more sophisticated lens design (similar in concept to *etendue*).

### Standard focus range

From Sheppard 1991, equation 18 proposes that in a medium of refractive index  $n_1$ , the maximum acceptable wavefront aberration (Rayleigh criterion) will not be exceeded if the thickness of a slab of dielectric  $t$  and refractive index  $n_2$  meets the following condition:

$$t \leq \frac{\lambda n_2^3}{2n_1^2(n_2^2 - n_1^2) \sin^4(\alpha/2)} \quad (a7)$$

where  $\alpha$  is the collection half-angle in the  $n_1$  space (i.e. the immersion). Originally evaluated for a phase error of  $\pi/2$ , equation (1) gives negative values for  $n_1 > n_2$ . If we allow  $n_1 > n_2$  and a phase error of  $\pm\pi/2$  then we can rewrite (1) in a slightly more convenient format to give the maximum depth of standard focus  $z_{sf\_max}$ :

$$z_{sf\_max} = \frac{\lambda}{2 \sin^4(\theta_i/2)} \left| \frac{n_s^3}{n_i^2(n_s^2 - n_i^2)} \right| \quad (a8)$$

### Remote refocus range

From [Botcherby 2007](#), equation 23 proposes that the Strehl ratio  $S$  of a remote refocus can be modelled by:

$$S = 1 - \frac{4n^2 k^2 z^4 (3 + 16 \cos \alpha + \cos 2\alpha) \sin^8(\alpha/2)}{75 f^2 (3 + 8 \cos \alpha + \cos 2\alpha)} \quad (\text{a9})$$

where  $n$  is the refractive index of the sample,  $k = 2\pi/\lambda$  is the wavenumber,  $z$  is the axial distance from the traditional focal plane,  $f$  is the focal length and  $\alpha$  is the collection half-angle of the objective. If we set  $S = 0.8$  (the traditional diffraction limit) and rearrange we can estimate the maximum remote refocus depth  $z_{rr, max}$ :

$$z_{rr\_max} = \pm \frac{1}{2 \sin^2(\theta_s/2)} \sqrt[4]{\frac{15\lambda^2 f^2 (3 + 8 \cos \theta_s + \cos 2\theta_s)}{\pi^2 n_s^2 (3 + 16 \cos \theta_s + \cos 2\theta_s)}} \quad (\text{a10})$$

Note: the substitution  $\alpha = \theta_s$  is subtle. In [Botcherby 2007](#) at the critical substitution of equation 8 ( $\sin \theta = \rho \sin \alpha$ ) the paper reads "In this expression  $\alpha$  is the semi-aperture acceptance angle of the lens" so one could assume  $\alpha = \theta_i$ . However the substitution is in reference to coordinates in *object space*.

### Combined range

For a microscope with remote refocus optics (e.g. Figure 2) we can now estimate the maximum focus range in the sample  $z_{max}$  as the sum of the standard and remote ranges:

$$z_{max} \approx z_{sf\_max} + |z_{rr\_max}| \quad (\text{a11})$$

Note: the *approximately* equals sign. The standard focus and remote refocus ranges use different definitions for the diffraction limit, and are approximate models that ignore higher order aberrations. There is also no consideration given to field effects, chromatic aberrations or design and manufacturing imperfections that can be expected in real objective lenses.

## Objective selection

In a SOLS microscope [Millet-Sikking 2019], as the angular range in the sample  $\theta_s$  decreases, the tilt of the last microscope  $\theta_{tilt}$  increases according to:

$$\theta_{tilt} = 90 - \theta_s \quad (deg) \quad (a13)$$

Currently the AMS-AGY v2.0 objective [Yang 2022] has the most extreme tilt range of any SOLS compatible objective, with maximum tilt of 55 degrees. So combining  $(a1)$ ,  $(a12)$  and  $(a13)$  the minimum acceptable sample space NA is:

$$NA_s \geq 1.33 \sin(90 - 55) = 0.76 \quad (\text{a14})$$

After applying the lower bound on NA of 0.76, the 'best' objectives for the standard immersions were selected in the following 2 categories:

- **Nikon objectives, highest NA:**

--	--	--	--	--	--	--	--

Part #	M	NA	Imm.	WD ( $\mu\text{m}$ )	FOV ( $\mu\text{m}$ )	$r_{\min}$ ( $\mu\text{m}$ )	N_px
MRD70470	40x	0.95	air	210	500	0.342	2927
MRY10060	60x	1.27	water	180	333	0.256	2608
MRD73950	100x	1.35	silicone	310	200	0.240	1663
MRD71970	100x	1.45	oil	130	200	0.224	1787

- **Nikon objectives, most pixels:**

Part #	M	NA	Imm.	WD ( $\mu\text{m}$ )	FOV ( $\mu\text{m}$ )	$r_{\min}$ ( $\mu\text{m}$ )	N_px
MRD70270	20x	0.80	air	800	1000	0.406	4930
MRD77200	20x	0.95	water	990	1000	0.342	5854
MRD73250	25x	1.05	silicone	550	800	0.309	5176
MRH01401	40x	1.30	oil	240	500	0.250	4005

Note: Speciality objectives in the categories of TIRF and Multi-photon may not perform optimally for remote refocus and were avoided.

## Zoom lens

In our previous remote refocus designs we used static lenses to adjust the magnification between the sample and the remote space according to equation 2 [Millett-Sikking 2018, Millett-Sikking 2019]. Specifically we chose to modify the second tube lens in the optical train, often referred to as 'tube lens 2' or TL2. The TL2 location is convenient, as it leaves the first objective and tube lens pair in their traditional (stock) configuration, and allows the addition of a unity magnification scanning system. Here we take the same approach, and optimize our zoom optics at the TL2 location, specifying some of the upstream and downstream optics in order to produce a concrete design.

### Specifications

To produce an inexpensive zoom lens with stock parts we narrow the optical requirement to a specific RR system. We assume a widefield microscope at 40x magnification since this offers many attractive primary objective options (air, water, silicone and oil immersion at high NA from various manufacturers). We then assume a 5mm focal length air lens for the second RR objective (often referred to as 'objective 2' or O2). For example the Nikon 40x0.95 air lens (9.5mm back focal plane diameter) is a good high NA option, with a high enough collection cone ( $\sim 72^\circ$ ) and pixel count ( $\sim 2927$ ) for most RR designs. We target a RR magnification that covers the full biological refractive index range (1.33-1.51) by tuning the focal length of TL2 in the range 150-132.5mm (i.e. 30-26.5x for microscope 2). Finally we assume a standard sCMOS field of view ( $\sim 13.5\text{mm}$  width) and add the additional constraints of needing a constant track length and telecentric image.

## Design

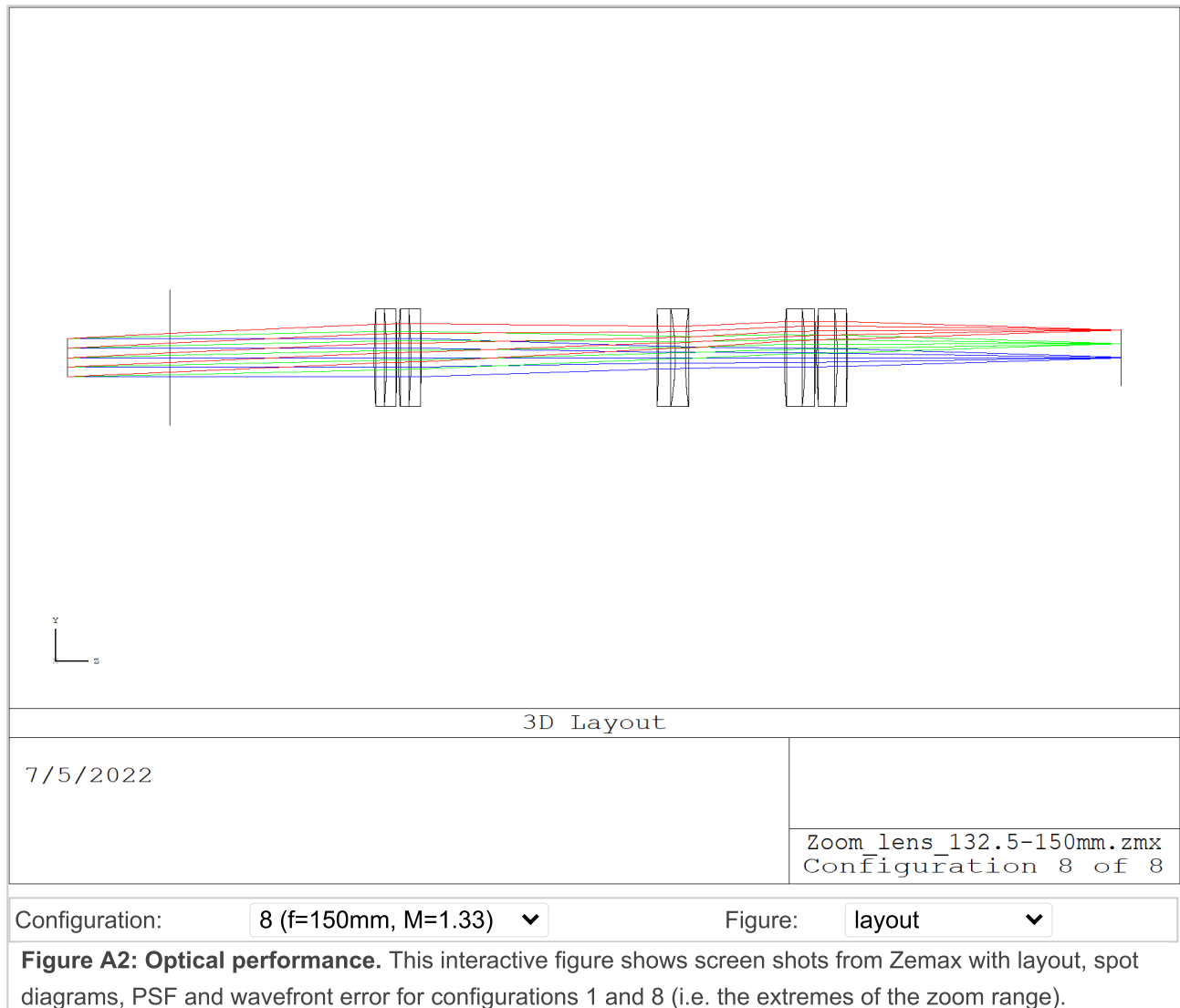
Using the above specifications, we adopt a simple 'positive-negative-positive' (PNP) zoom design and cycle through readily available stock parts. After some iteration we settle on a series of Edmund Optics achromats that satisfy our optical requirements, whilst also being mechanically compatible and inexpensive (see the [mechanics section](#) for parts). Our constraint of only using stock lenses forces a 5 achromat solution ([Figure A2](#)), where a 3 achromat custom design would suffice. We note that a 'standard' tube lens typically has 2 achromats, so a 3 lens solution would only add 1 achromat to the optical train (a minimal drawback for the system). However, we consider the small penalty on transmission efficiency ( $\sim 1.5\%$ ) from the 2 additional achromats in the design we present to be a good trade for avoiding bespoke glass.

## Performance

In [Figure A1](#) we see the spot diagrams as a function of field (centre to edge) and configuration (min to max focal length) across the visible spectrum (450-700nm). We can see that the system is mostly diffraction limited throughout the matrix, with some marginal degradation at the edge of the field for the shorter focal lengths (higher RR magnifications). In the interactive [Figure A2](#) we show detailed views of the performance at the extremes of the range with configurations 1 and 8 (i.e. magnifications of 1.33 and 1.51). See the zoom lens 'optics' folder for more details (including Zemax files).



**Figure A1: Multi-configuration spot diagram.** This screen shot from Zemax shows the spot diagrams as a function of field (0, 1.3 and 2.6deg) and configurations (1-8) across the visible spectrum (450-700nm). Here the configurations 1 to 8 correspond to target focal lengths of 132.5mm to 150mm in steps of 2.5mm. Spots that appear within the Airy diameter (black ring) can be considered diffraction limited.



## Motion

Part of the design challenge in a zoom system is accommodating the motion of elements (or groups of elements). Here we adopt relatively large motions of 2 of the 3 lens groups from the PNP design. This has the drawback of being slower than small motions, but the benefit of loosening the opto-mechanical tolerances of the system, thereby allowing us to use stock optics and mechanics. In [Figure A3](#) we see how we need to move the lens groups from the 'zero position' with a focal length of 132.5mm to the 'limit position' with a focal length of 150mm. The negative lens (centre element in the design) moves the most by almost 50mm, while the positive group near the image move slightly less by around 42mm (the first lens group in the design is static).

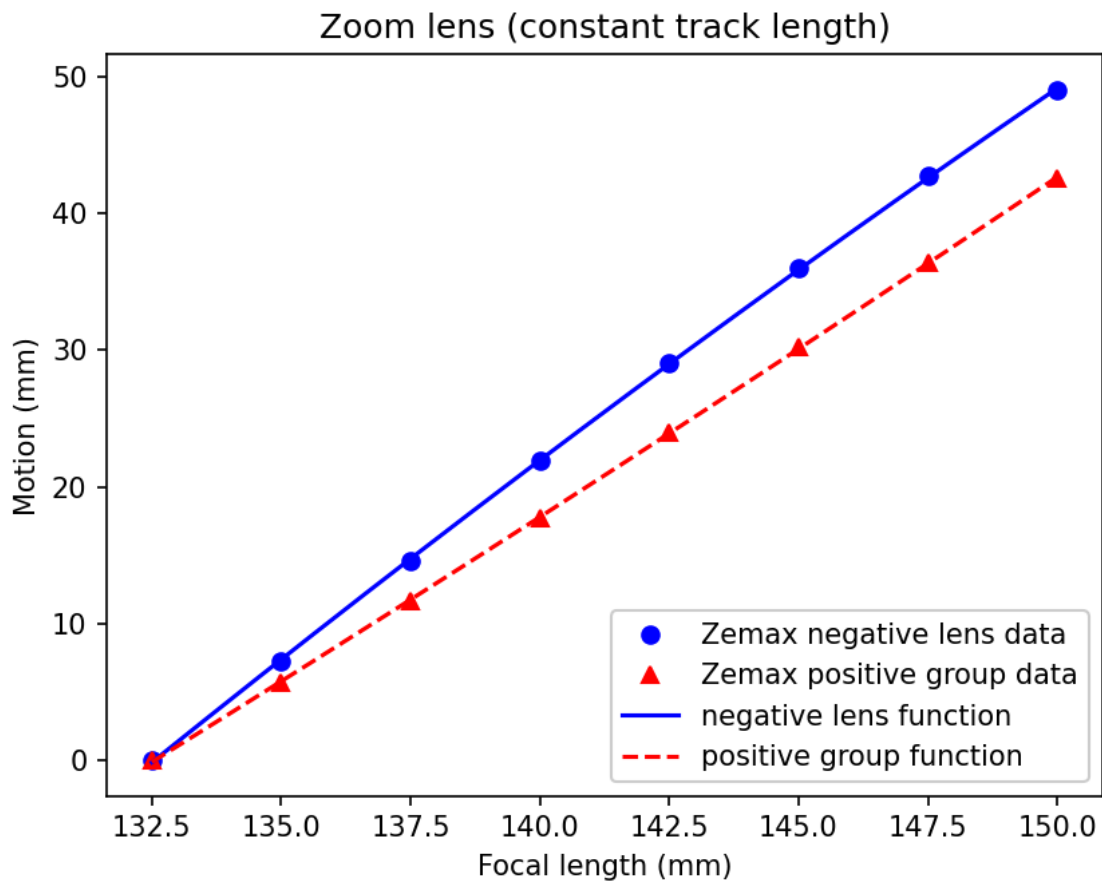


**Figure A3: Zoom lens motion.** This plot shows how the negative lens (central element in the PNP design) and positive group (2 achromats near the image) should move to produce a given focal length for the zoom lens. The first lens group in the PNP design is static.

Below we provide the 'motion functions' that convert a requested focal length to a required movement of each lens or lens group (for driving linear stages or equivalent mechanics). Here's [an example](#) for a focal length of 140mm:

```
# Zoom_lens_132.5-150mm_motion.ods trendline polynomials
# Data from Zemax
def negative_lens_motion(f_mm):
    motion_mm = (- 0.012921858472509 * f_mm**2
                  + 6.467807910667240 * f_mm
                  - 630.2815284192340)
    return motion_mm

def positive_group_motion(f_mm):
    motion_mm = (+ 0.005518525287293 * f_mm**2
                  + 0.885914869404723 * f_mm
                  - 214.4010550854960)
    return motion_mm

# Input:
```

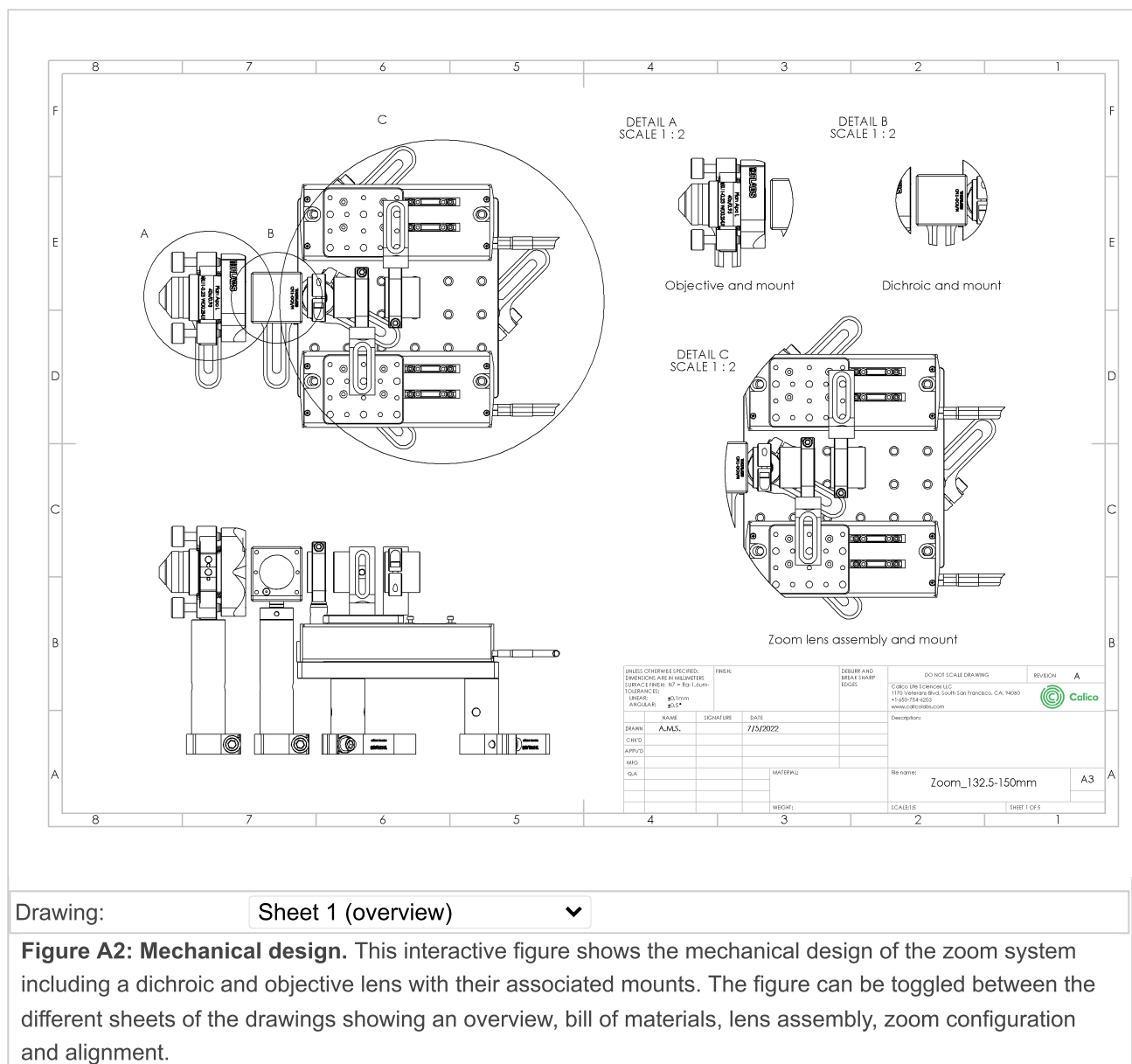
```
f_mm = 140
N_motion = negative_lens_motion(f_mm)
P_motion = positive_group_motion(f_mm)
print('requested focal length = %0.2f'%f_mm)
print('negative lens motion    = %0.2f'%N_motion)
print('positive group motion   = %0.2f'%P_motion)

# Output:
## requested focal length = 140.00
## negative lens motion    = 21.94
## positive group motion   = 17.79
```

## Mechanics

Here we offer a relatively simple mechanical design ([Figure A4](#)), that utilizes some fast 50mm linear stages from Thorlabs (DDS050). However, any mechanical solution that achieves the required alignment of the lenses and relative motions is acceptable. The solution we present combines the zoom optics into a single large mount that can (in principle) be aligned to an axis that is parallel to the optical table, and includes provision for an objective, a dichroic and an unhampered image plane. The DDS050 stages have a max speed of 500mm/s so we can expect a responsive zoom experience for tuning the magnification to different sample types. See the included [Zoom\\_lens\\_132.5-150mm.pdf](#) for a high quality reproduction, or the '[mechanics](#)' folder for more details (including CAD files).





## References

- [Pawley 2006] Handbook of Biological Confocal Microscopy, third edition; J. Pawley; Springer US, ISBN 978-0-387-25921-5, eBook ISBN 978-0-387-45524-2, (2006) <https://doi.org/10.1007/978-0-387-45524-2>
- [Sheppard 1991] Effects of aberrating layers and tube length on con focal imaging properties; C. Sheppard and C. J. Cogswell; Optik, vol 87(1), p34-38, (1991)  
[https://www.researchgate.net/publication/235927740\\_Effects\\_of\\_aberrating\\_layers\\_and\\_tube\\_length\\_on\\_c\\_on\\_focal\\_imaging\\_properties](https://www.researchgate.net/publication/235927740_Effects_of_aberrating_layers_and_tube_length_on_c_on_focal_imaging_properties)
- [Botcherby 2007] An optical technique for remote focusing in microscopy; E.J. Botcherby, R. Juškaitis, M.J. Booth and T. Wilson; Optics Communications, vol 281(4), p880-887, (2007)  
<https://doi.org/10.1016/j.optcom.2007.10.007>
- [Millett-Sikking 2019] High NA single-objective light-sheet; A. Millett-Sikking, K.M. Dean, R. Fiolka, A. Fardad, L. Whitehead and A.G. York; (2019) <https://doi.org/10.5281/zenodo.3244420>

5. [Yang 2022] DaXi—high-resolution, large imaging volume and multi-view single-objective light-sheet microscopy; B. Yang, M. Lange, A. Millett-Sikking, X. Zhao, J. Bragantini, S. VijayKumar, M. Kamb, R. Gómez-Sjöberg, A.C. Solak, W. Wang, H. Kobayashi, M.N. McCarroll, L.W. Whitehead, R.P. Fiolka, T.B. Kornberg, A.G. York and L.A. Royer; (2022) <https://doi.org/10.1038/s41592-022-01417-2>
6. [Millett-Sikking 2018] Remote refocus enables class-leading spatiotemporal resolution in 4D optical microscopy; A. Millett-Sikking, N.H. Thayer, A. Bohnert and A.G. York; (2018) <https://doi.org/10.5281/zenodo.1146083>



Hosted on

[GitHub Pages](#)